Deakin Research Online

This is the published version:

Barbante, Gregory J., Hogan, Conor F., Wilson, David J. D., Lewcenko, Naomi A., Pfeffer, Frederick M., Barnett, Neil W. and Francis, Paul S. 2011, Simultaneous control of spectroscopic and electrochemical properties in functionalised electrochemiluminescent tris(2,2'-bipyridine)ruthenium(II) complexes, *Analyst*, vol. 136, no. 7, pp. 1329-1338.

Available from Deakin Research Online:

http://hdl.handle.net/10536/DRO/DU:30040489

Reproduced with the kind permission of the copyright owner.

Copyright: 2011, Royal Society of Chemistry.

Analyst

View Online / Journal Homepage / Table of Contents for this issue
Dynamic Article Links

Cite this: *Analyst*, 2011, **136**, 1329

www.rsc.org/analyst

PAPER

Simultaneous control of spectroscopic and electrochemical properties in functionalised electrochemiluminescent tris(2,2′-bipyridine)ruthenium(II) complexes†

Gregory J. Barbante,[a] Conor F. Hogan,*[a] David J. D. Wilson,[a] Naomi A. Lewcenko,‡[b] Frederick M. Pfeffer,[b] Neil W. Barnett[b] and Paul S. Francis*[b]

Received 27th November 2010, Accepted 6th January 2011
DOI: 10.1039/c0an00952k

Published on 04 February 2011 on http://pubs.rsc.org | doi:10.1039/C0AN00952K
Downloaded by Deakin University on 03 January 2012

Using a combination of electrochemical, spectroscopic and computational techniques, we have explored the fundamental properties of a series of ruthenium diimine complexes designed for coupling with other molecules or surfaces for electrochemiluminescence (ECL) sensing applications. With appropriate choice of ligand functionality, it is possible to manipulate emission wavelengths while keeping the redox ability of the complex relatively constant. DFT calculations show that in the case of electron withdrawing substituents such as ester or amide, the excited state is located on the substituted bipyridine ligand whereas in the case of alkyl functionality it is localised on a bipyridine. The factors that dictate annihilation ECL efficiency are interrelated. For example, the same factors that determine ΔG for the annihilation reaction (*i.e.* the relative energies of the HOMO and LUMO) have a corresponding effect on the energy of the excited state product. As a result, most of the complexes populate the excited state with an efficiency (Φ_{ex}) of close to 80% despite the relatively wide range of emission maxima. The quantum yield of emission (Φ_p) and the possibility of competing side reactions are found to be the main determinants of ECL intensity.

Introduction

Amongst their many important applications,[1–3] ruthenium polypyridine complexes have been widely used for photoluminescence, chemiluminescence (CL) and electrochemiluminescence (ECL) analysis.[4–6] Although the majority of these studies have focussed on tris(2,2′-bipyridine)ruthenium(II) ($Ru(bpy)_3^{2+}$) (see Fig. 1 for ligand structures), a wide range of analogues and derivatives have been explored,[5–7] to modify the chemical or spectroscopic properties, immobilise the complex, or to bind it to specific functionality to create new avenues for chemical measurement, such as the synthesis of ECL labels for immunoassay or luminescent hosts for anion sensing.

The characteristic orange photoluminescence from $Ru(bpy)_3^{2+}$ results from the excitation of an electron from the metal-based $d(\pi_M)$ orbitals to the ligand-based π^* antibonding orbitals—a metal-to-ligand charge-transfer (MLCT)—followed by inter-system crossing to the lowest triplet state, from where the emission occurs.[6,8] The same MLCT state may be attained in CL or ECL reactions if an electron is transferred from a powerful reductant derived from the analyte/co-reactant to the π^* orbital of a bipyridine ligand of $Ru(bpy)_3^{3+}$.[6]

The addition of electron withdrawing groups on the ligands of $Ru(bpy)_3^{2+}$ causes a red-shift in the emission spectrum, by lowering the π^* energy levels.[9] Ligands that have electron-donating substituents (such as methyl groups) can also lower the energy of the radiative transition, because the extra electron density destabilises the d (HOMO) orbital in the ground state species, reducing the energy gap to the π^* level of the charge-acceptor bipyridine ligands.[9–11] However, a clear understanding of the extent that different functional groups influence the spectral distribution has been hampered by the disparity of conditions (solvent, reference electrode, concentration of the complex, the number of derivatised ligands on each complex) between studies, and the frequent use of uncorrected emission spectra,[9–15] which is particularly problematic for species that emit above 600 nm, where there is significant changes in the relative response of many photomultiplier tubes.

The work presented here was motivated by our interest in developing ECL and CL based sensing materials with varying emission wavelengths for potential applications in multiplexed

[a]*Department of Chemistry, La Trobe Institute for Molecular Science, La Trobe University, Victoria, 3086, Australia. E-mail: c.hogan@latrobe.edu.au; Tel: +61 3 9479 3747*
[b]*School of Life and Environmental Sciences, Deakin University, Geelong, Victoria, 3217, Australia. E-mail: psf@deakin.edu.au; Tel: +61 3 5227 1294*

† Electronic supplementary information (ESI) available: Comparison of HOMO–LUMO gap (H-L) calculated by DFT and time dependent (TD) DFT with experimental data, and Mulliken population analysis of frontier molecular orbitals. See DOI: 10.1039/c0an00952k

‡ Current address: School of Chemistry, Monash University, Clayton, Victoria 3800, Australia.

Published on 04 February 2011 on http://pubs.rsc.org | doi:10.1039/C0AN00952K
Downloaded by Deakin University on 03 January 2012

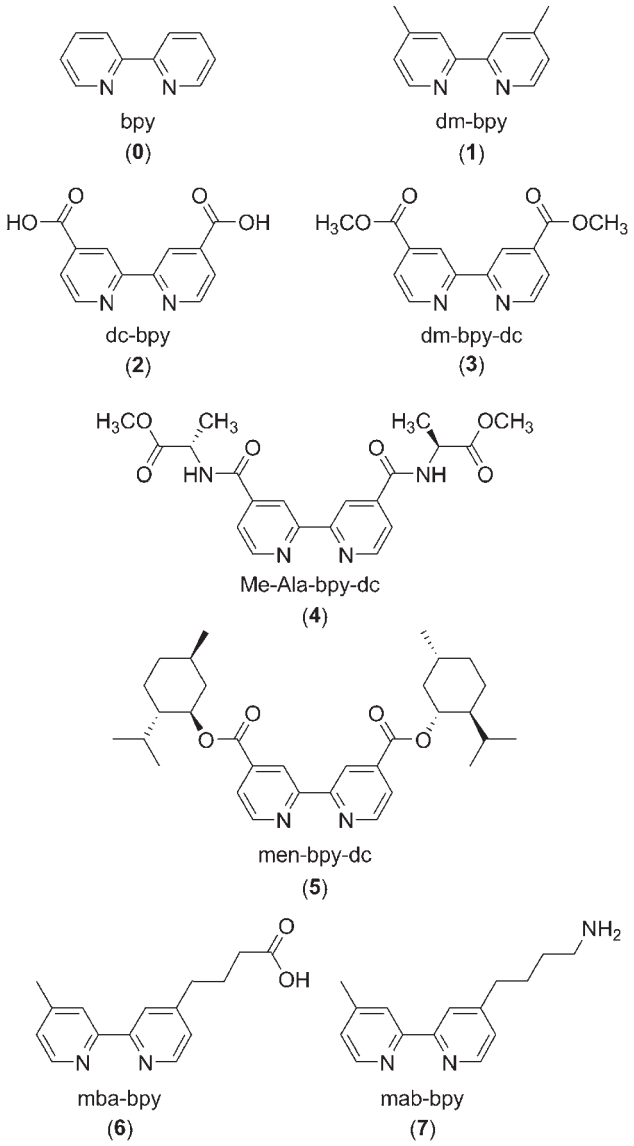

Fig. 1 Ligands selected for comparison (within heteroleptic $[Ru(bpy)_2(L)]^{2+}$ complexes denoted by the number below each ligand): 2,2′-bipyridine (bpy); 4,4′-dimethyl-2,2′-bipyridine (dm-bpy); 2,2′-bipyridine-4,4′-dicarboxylic acid (dc-bpy); dimethyl 2,2′-bipyridine-4,4′-dicarboxylate (dm-bpy-dc); bis((1*R*,2*S*,5*R*)-2-isopropyl-5-methylcyclohexyl) 2,2′-bipyridine-4,4′-dicarboxylate (men-bpy-dc); N^4,$N^{4'}$-bis((2*S*)-1-methoxy-1-oxopropan-2-yl) 2,2′-bipyridyl-4,4′-dicarboxamide (Me-Ala-bpy-dc); 4′-methyl-2,2′-bipyridine-4-butanoic acid (mba-bpy); and 4-methyl-4′-aminobutyl-2,2′-bipyridine (mab-bpy).

sensing as well as the ability to be coupled to target analytes or electrode surfaces. Such applications require careful control over often opposing redox, spectroscopic and physical properties. Because the ECL or CL process is typically complex, spectroscopic or electrochemical information cannot be used in isolation to predict ECL or CL intensity. For example, tris(2-phenylpyridine)iridium(III), which has a photoluminescence quantum yield of 97% in oxygen-free solvent,[16] was investigated as a promising ECL emitter. However, its favourable photophysical properties did not translate into analytically useful ECL because the oxidation potential (~0.55 V *vs.* ferrocene[17]) is too low to give efficient co-reactant ECL. On the other hand, if the oxidation potential of a complex is too high, parasitic side reactions may degrade the sensitivity or selectivity of the ECL assay.[18]

In this study, we compare the spectroscopy, electrochemistry and ECL of tris(2,2′-bipyridine)ruthenium(II) derivatives containing one ligand with chemical functionality that has commonly been used to either modify the characteristics of the parent complex or link it with other species. One such ligand is 4,4′-dimethyl-2,2′-bipyridine (dm-bpy). Numerous researchers have examined the influence of this simple electron-donating substituent on the fundamental properties (such as electron localisation, photoluminescence quantum yields, and ECL intensities) of ruthenium polypyridine complexes.[9,10,19,20] Longer alkyl groups have been used to provide space between the ruthenium complex and functionality used for labelling or immobilisation[21,22] or link multiple ruthenium complexes.[23] We have therefore included 4-methyl-4′-aminobutyl-2,2′-bipyridine (mab-bpy) and 4′-methyl-2,2′-bipyridine-4-butanoic acid (mba-bpy), which have previously been utilised as ECL labels[24] and in the synthesis of ECL dendrimers.[25,26]

The influence of electron-withdrawing substituents on the physical and photophysical properties of ruthenium complexes containing 2,2′-bipyridine-4,4′-dicarboxylic acid (dc-bpy) has also been explored by numerous researchers.[9,11,27–29] Moreover, there has been considerable interest in ruthenium complexes containing this ligand as components of dye-sensitised solar cells, because the carboxylate groups provide a convenient point of attachment to TiO_2 semiconductors.[30,31] The esterification of 2,2′-bipyridine-4,4′-dicarboxylic acid has been used to develop ligands that further modify the properties of the complex,[14,32] introduce new structures (such as labelling groups,[33] hydrophobic alkyl chains[34] and chiral functionality[35,36]) and form electrochemiluminescent metallodendrimers.[37] Ruthenium complexes incorporating the dimethyl ester of 2,2′-bipyridine-4,4′-dicarboxylic acid (dm-bpy-dc) have been used in solid-state light-emitting devices, because the esterified ligands result in a more "technologically useful" red luminescence (λ_{max} = 690 nm) compared to the red-orange emission of $Ru(bpy)_3(PF_6)_2$.[38] For the current investigation, we have prepared the dimethyl ester (dm-bpy-dc), and di-(1*R*,2*S*,5*R*)-menthyl ester (men-bpy-dc) derivatives of 2,2′-bipyridine.

The formation of amides by combining 2,2′-bipyridine-4,4′-dicarboxylic acid with derivatised amino acids is another convenient approach to manipulate the exterior structure of ruthenium polypyridine complexes, which has been exploited for the development of photoinduced electron transfer agents.[39,40] More generally, ligands with an amide group adjacent to the bipyridine ring have been incorporated into ruthenium complexes for the development of ECL dendrimers,[26] immobilised CL and ECL reagents[41,42] and anion sensors,[43] and to introduce chiral functionality[44] or other groups that modify the properties of the complex.[31] We have included a complex containing a 2,2′-bipyridyl-4,4′-dicarboxamide ligand (Me-Ala-bpy-dc) prepared using the methyl ester of L-alanine, to examine the influence of amide functionality.

Experimental

General instrumentation

^1H and ^{13}C NMR spectra were obtained using 270 MHz and 400 MHz JEOL Eclipse spectrometers. Chemical shifts (δ) are

 This journal is © The Royal Society of Chemistry 2011

reported in ppm and referenced against tetramethylsilane (TMS). Signal multiplicities were assigned as singlet (s), doublet (d), triplet (t), quartet (q), doublet of triplets (dt), multiplet (m) and broad (br). Melting points (uncorrected) were established using a Reichert hot stage microscope.

Mass spectra were obtained using a Platform II single quadrupole mass spectrometer (Micromass, Altrincham, UK). High-resolution mass spectra were obtained using a 6210 MSDTOF mass spectrometer (Agilent Technologies, Forest Hill, VIC, Australia) with the following conditions: drying gas, nitrogen (7 mL min^{-1}, 350 °C); nebuliser gas, nitrogen (16 psi); capillary voltage, 4.0 kV; vaporiser temperature, 350 °C; and cone voltage, 60 V. Samples were prepared in acetonitrile, unless otherwise stated.

Absorption and emission spectra

UV-visible absorbance spectra were collected using a Cary 300 Bio UV-Vis spectrophotometer (Varian Australia, Mulgrave, VIC, Australia) with 1 cm path length quartz cells. Photoluminescence spectra were collected with a Cary Eclipse Spectrofluorimeter (Varian Australia, Mulgrave, VIC, Australia) with an R928 photomultiplier tube (Hamamatsu, Iwata-gun, Shizuoka-ken, Japan), using a 1 cm quartz cuvette (5 nm band pass, 1 nm data interval, PMT voltage: 800 V). Emission spectra correction factors were established using an Optronic Laboratories spectral irradiance standard (model OL 245M) with constant current source (model OL 65A).

Photoluminescence quantum yields (Φ_p) were measured with reference to the following equation:

$$\Phi_x = \Phi_{ref}\,(Grad_x/Grad_{ref})(\eta_x^2/\eta_{ref}^2) \quad (1)$$

where Φ_{ref} is the quantum yield of the reference complex, $[Ru(bpy)_3][PF_6]_2$ (0.062 in CH_3CN);[45] x denotes sample and ref is the reference; *Grad* is the gradient of the *absorbance vs. integrated emission intensity* graph, using at least five different concentrations with absorbance below 0.1 and achieving R^2 close to 1; η is the refractive index of the solvent used. Quantum yield determinations were conducted at room temperature (21 ± 3 °C). All solutions were thoroughly degassed with nitrogen in septum sealed quartz cells prior to measurements.

Cyclic voltammetry and electrochemiluminescence

Electrochemical experiments were performed using μAUTOLAB type II electrochemical station potentiostat (MEP Instruments, North Ryde, NSW, Australia) with General Purpose Electrochemical Systems (GPES) software (version 4.9). The electrochemical cell consisted of a glass cell with a quartz window base and Teflon cover with spill tray. The cell was encased in a custom-built light-tight faraday cage. A conventional three-electrode configuration, consisting of a glassy carbon 3 mm diameter working electrode, shrouded in Teflon (CH Instruments, Austin, TX, USA), a 1 cm^2 platinum gauze auxiliary electrode and a silver wire quasi reference electrode. Potentials were referenced to the ferrocene/ferrocenium couple measured *in situ* (1 mM) in each case.

For the measurement of ECL, a photomultiplier tube (model 98285B; Electron Tubes, Ruislip, UK), biased at 500 V using a PM28B power supply (Electron Tubes), was mounted against the quartz window base of the custom-built electrochemical cell. The output signal from the photomultiplier was acquired using the auxiliary channel of the potentiostat *via* a custom made preamplifier. ECL spectra were obtained using an Ocean Optics CCD, model QE65000, UV/VIS fibre optic (length 1.00 metre) and the acquisition was triggered using a HR 4000 Break-Out box in conjunction with the PGstat 12 AUTOLAB potentiostat.

Solution phase ECL efficiencies (ϕ_{ECL}) were evaluated using the equation:

$$\phi_{ECL} = \phi^\circ_{ECL}\,(IQ^\circ_f/Q_fI^\circ) \quad (2)$$

where ϕ°_{ECL} is the ECL efficiency of the standard, (1 mM $Ru(bpy)_3^{2+}$ and 0.1 M $[Bu_4N][PF_6]$ in acetonitrile) taken as 5.0%,[46] I and I° are the integrated PMT responses for the sample and the standard respectively, and Q_f and Q°_f are the faradaic charges passed for the sample and standard respectively.

The potentials used to generate the 3+ and 1+ forms of the ruthenium complex in the annihilation reaction were obtained from the cyclic voltammograms. The cathodic and anodic potentials were stepped for 1.0 s and the ECL chronoamperometry experiments underwent 10 cycles. Φ_{ECL} values measured using the CCD and PMT were identical within experimental error.

The ruthenium complexes were prepared at a concentration of 1 mM in freshly distilled acetonitrile, with 0.1 M tetrabutylammonium hexafluorophosphate ($TBAPF_6$) as the supporting electrolyte. Prior to each experiment, the working electrode was polished using 0.3 μm and then 0.05 μm alumina with water on a felt pad, sonicated in MilliQ water (1 min), rinsed in freshly distilled acetonitrile and dried with a stream of nitrogen. The working electrode was then positioned at an appropriate distance (~2 mm) from the bottom of the cell for detection of the ECL signal, and the solution was purged with nitrogen for 10–15 min. All solutions were scanned between 1.6 V and −2.5 V with an initial potential of 0 V. Scan rates ranging from 0.01 to 0.5 V s^{-1} were used in cyclic voltammetry to evaluate diffusion coefficients (D) using the Randles–Sevcik equation.

Computational methods

Density functional theory (DFT) calculations were carried out within the Gaussian 09 suite of programs.[47] Geometries were optimised in the absence of solvent with the B3LYP[48–50] and mPW1PW91[51,52] functionals, with both yielding similar structures. Only mPW1PW91 results are presented, since it has been shown previously that this functional yields reliable results.[53] Symmetry of the optimised structures was D_3 (**0**), C_2 (**1–3**) and C_1 (**4–7**). Three metal effective-core potential (ECP) basis sets were considered for geometry optimisations and molecular orbital (MO) calculations: LANL2MB,[54–56] LANL2DZ,[56,57] and SDD.[57,58] In each case the 6-31 + G(d) basis set[59–61] was used for all non-metal atoms. Final single-point energy calculations were carried out at the SDD/6-31 + G(d) optimised geometries using the SDD basis for Ru and the TZVP basis set[62,63] for all other atoms. The polarisable continuum model (PCM)[64] was used to model solvent effects at the gas-phase optimised geometries with a solvent of acetonitrile. Calculations with water solvent

Published on 04 February 2011 on http://pubs.rsc.org | doi:10.1039/C0AN00952K
Downloaded by Deakin University on 03 January 2012

produced almost identical results and so only results including solvation by acetonitrile are presented here. HOMO and LUMO energies were calculated using DFT MOs, as well as with time-dependent DFT (TD-DFT)[65] using the SDD/TZVP basis sets, which may be expected to yield more accurate and reliable LUMO energies. SCF convergence criteria of 10^{-8} a.u. were employed throughout. Molecular orbital analysis was carried out with the AOMix program.[66]

Synthesis and characterisation of derivatised ligands

4,4′-Dimethyl-2,2′-bipyridine (dm-bpy) was prepared from 4-methylpyridine (93.33 g, 1.00 mol) using a RANEY® nickel catalyst.[67,68] The crude product was recrystallised from toluene to yield white crystals (15.2 g, 82.5 mmol, 12% yield, mp 168–171 °C, lit.,[68] 171–172 °C). ^{1}H NMR ($CDCl_3$) δ: 2.47 (6H, s, CH_3), 7.11 (2H, d, H5), 8.21 (2H, s, H3), 8.51 (2H, d, H6). ^{13}C NMR ($CDCl_3$) δ: 21.24 (CH_3), 122.07 (C5), 124.70 (C3), 148.20 (C4), 148.98 (C6), 156.10 (C2) (assignments based on those reported for 4,4′-dimethyl-2,2′-bipyridine in the Spectral Database for Organic Compounds SDBS[69]).

2,2′-Bipyridine-4,4′-dicarboxylic acid (dc-bpy) was prepared by reacting 4,4′-dimethyl-2,2′-bipyridine (5.00 g, 27.1 mmol) with potassium dichromate (36 g), as described by Oki and Morgan.[70] 6.49 g, 26.6 mmol, 98% yield, mp >400 °C (dec.). ^{1}H NMR (TFA) δ: 8.81 (2H, d, H5), 9.38 (2H, d, H6), 9.49 (2H, s, H3) (assignments based on those by Launikonis and co-workers[71]). *m*/*z* ($M + H^+$) calculated: 245.0557; found: 245.0547.

The dimethyl dicarboxylate (dm-bpy-dc), dimenthyl dicarboxylate (men-bpy-dc), and bis(L-alanine methyl ester) dicarboxamide (Me-Ala-bpy-dc) derivatives were prepared from the 2,2′-bipyridine-4,4′-dicarboxylic acid *via* the corresponding dicarbonyl dichloride, based on the procedure described by Sprintschnik and co-workers[72] with some modifications.

To prepare dimethyl 2,2′-bipyridine-4,4′-dicarboxylate (dm-bpy-dc), the corresponding diacid (1.00 g, 4.09 mmol) was suspended in thionyl chloride ($SOCl_2$; 15 mL) and heated at 100 °C (15 min) then cooled to room temperature. One drop of DMF was added and the mixture was again refluxed (2 h) then allowed to cool. The $SOCl_2$ was removed under reduced pressure and the resultant orange solid dried *in vacuo* at 30 °C (2 h). The crude product was combined with dry methanol (50 mL), refluxed for 2 h and cooled to room temperature. Chloroform ($CHCl_3$; 200 mL) was added and the resulting suspension filtered. The filtrate was transferred to a separating funnel and washed with cold aqueous sodium hydrogen carbonate ($NaHCO_3$; 100 mL), and saturated NaCl solution (2 × 200 mL), then dried ($MgSO_4$) and the solvent removed under reduced pressure to yield a yellow oil. The product solidified upon addition of a minimum volume of pet. spirit (40–60 °C). Recrystallisation from toluene (twice) then drying *in vacuo* afforded a white crystalline solid (641 mg, 2.34 mmol, yield 57%, mp 207–210 °C, lit.,[73] 208–210 °C). ^{1}H NMR ($CDCl_3$) δ: 4.00 (6H, s, OCH_3), 7.89 (2H, d, H5), 8.86 (2H, d, H6), 8.95 (2H, s H3). ^{13}C NMR ($CDCl_3$) δ: 52.8 (OCH_3), 120.7 (C3), 123.3 (C5), 138.7 (C4), 150.2 (C6), 156.6 (C2), 165.7 (carbonyl) (assignments were verified using a GHMBC experiment and the shifts were in good agreement with those reported by Oki and Morgan[70]). *m*/*z* ($M + H^+$) calculated: 273.0870; found: 273.0857.

In a similar manner, bis((1*R*,2*S*,5*R*)-2-isopropyl-5-methylcyclohexyl) 2,2′-bipyridine-4,4′-dicarboxylate (men-bpy-dc) was prepared from the diacid (5.02 g, 20.6 mmol) by conversion to the dicarbonyl dichloride and reaction with menthol, using toluene as the solvent. 5.76 g, 11.1 mmol, yield 54%, mp 167–168 °C. ^{1}H NMR ($CDCl_3$) δ: 0.80 (6H, d), 0.94 (12H, t), 1.10–1.17 (6H, m), 1.58–2.17 (12H, m), 5.02 (2H, dt), 7.91 (2H, d), 8.87 (2H, d), 8.92 (2H, s). ^{13}C NMR ($CDCl_3$) δ: 16.38, 20.75, 22.00, 23.48, 26.43, 31.47, 34.18, 40.78, 47.03, 76.04, 120.72, 123.32, 139.46, 149.93, 156.32, 164.58. *m*/*z* ($M + H^+$) calculated: 521.7, found 521.7.

N^4,$N^{4\prime}$-Bis((2*S*)-1-methoxy-1-oxopropan-2-yl) 2,2′-bipyridyl-4,4′-dicarboxamide (Me-Ala-bpy-dc) was prepared from the diacid (972 mg, 3.98 mmol) by conversion to the dicarbonyl dichloride and reaction with L-alanine methyl ester hydrochloride (840 mg, 6.02 mmol), *N*,*N*′-dimethylformamide (DMF; 15 mL) and triethylamine (839 μL) at −20 °C. The mixture was allowed to warm to room temperature and stirred overnight prior to quenching with water (10 mL). The solution was filtered to remove unreacted starting material then the solvent was removed under reduced pressure. The crude product was dissolved in $CHCl_3$ (250 mL) and washed with 0.5 M HCl (200 mL) and the acid layer extracted with $CHCl_3$ (2 × 100 mL). The combined organic layers were washed with water (2 × 100 mL) and saturated NaCl solution (50 mL), dried using $MgSO_4$ and the solvent was removed under reduced pressure. The solid material was then recrystallised from ethyl acetate and dried *in vacuo* to yield white crystals (841 mg, 2.03 mmol, yield 51%, mp 240–242 °C). ^{1}H NMR ($CDCl_3$) δ: 1.58 (6H, d), 3.83 (6H, s), 4.85 (2H, dt), 7.03 (2H, d), 7.81 (2H, d), 8.74 (2H, s), 8.84 (2H, d). ^{13}C NMR ($CDCl_3$) δ: 18.49, 48.71, 52.75, 117.78, 122.16, 142.23, 150.21, 156.09, 164.83, 173.23.

Synthesis of ruthenium complexes

The *cis*-dichlorobis(2,2′-bipyridine)ruthenium(II) complex ($Ru(bpy)_2Cl_2\cdot 2H_2O$) was prepared by the method of Sullivan and co-workers.[74] The heteroleptic ruthenium complexes were prepared in a similar manner to that previously reported.[74,75] $Ru(bpy)_2Cl_2\cdot 2H_2O$ (250 mg, 0.480 mmol) in hot EtOH/H_2O (15 mL/25 mL) was combined with 1.5 molar equivalents of the respective derivatised bipyridine compound in hot EtOH (50 mL), and flushed with nitrogen gas for 15 min. The mixture was refluxed for three days and then cooled to room temperature. The volume was reduced by one third and a five molar excess of aqueous ammonium hexafluorophosphate (NH_4PF_6) was added. The precipitate was filtered, washed with water (2 × 50 mL), diethyl ether (2 × 50 mL) and dried *in vacuo* to yield a brown solid. The hexafluorophosphate salt of tris(2,2′-bipyridine)ruthenium(II) was prepared from $Ru(bpy)_3Cl_2\cdot 6H_2O$, which was purchased from Strem Chemicals (Massachusetts, USA). The identity of each complex was confirmed using high resolution mass spectrometry in the positive ion mode. In each case, the characteristic molecular isotopic distribution was observed.

Characterisation of ruthenium complexes

$Ru(bpy)_2(dm\text{-}bpy)(PF_6)_2$: 275 mg, 0.310 mmol, yield 64%, mp > 350 °C (dec.), *m*/*z* 299.0704 $[C_{32}H_{28}N_6Ru]^{2+}$ (calculated:

Published on 04 February 2011 on http://pubs.rsc.org | doi:10.1039/C0AN00952K
Downloaded by Deakin University on 03 January 2012

This journal is © The Royal Society of Chemistry 2011

Published on 04 February 2011 on http://pubs.rsc.org | doi:10.1039/C0AN00952K
Downloaded by Deakin University on 03 January 2012

299.0704), *m/z* 743.1018 $[C_{32}H_{28}N_6RuPF_6]^+$ (calculated: 743.1055) (**1**).

$Ru(bpy)_2(dc\text{-}bpy)(PF_6)_2$: 270 mg, 0.285 mmol, yield 59%, mp > 350 °C (dec.), *m/z* 329.0446 $[C_{32}H_{24}N_6O_4Ru]^{2+}$ (calculated: 329.0446), *m/z* 803.0508 $[C_{32}H_{24}N_6O_4RuPF_6]^+$ (calculated: 803.0544), *m/z* 657.0807 $[C_{32}H_{23}N_6O_4Ru]^+$ (calculated: 657.0819) (**2**).

$Ru(bpy)_2(dm\text{-}bpy\text{-}dc)(PF_6)_2$: 288 mg, 0.295 mmol, yield 61%, mp > 350 °C (dec.), *m/z* 343.0587 $[C_{34}H_{28}N_6O_4Ru]^{2+}$ (calculated: 343.0602), *m/z* 831.0793 $[C_{34}H_{28}N_6O_4RuPF_6]^+$ (calculated: 831.0857) (**3**).

$Ru(bpy)_2(Me\text{-}Ala\text{-}bpy\text{-}dc)(PF_6)_2$: 246 mg, 0.220 mmol, yield 46%, mp > 350 °C (dec.), *m/z* 414.0968 $[C_{40}H_{38}N_8O_6Ru]^{2+}$ (calculated: 414.0973), *m/z* 973.1552 $[C_{40}H_{38}N_8O_6RuPF_6]^+$ (calculated: 973.1600) (**4**).

$Ru(bpy)_2(men\text{-}bpy\text{-}dc)(PF6)_2$: 232 mg, 0.190 mmol, yield 39%, mp > 350 °C (dec.), *m/z* 467.1834 $[C_{52}H_{60}N_6O_4Ru]^{2+}$ (calculated: 467.1854), *m/z* 1047.3499 $[C_{52}H_{60}N_6O_4RuPF_6]^+$ (calculated: 1079.3356) (**5**).

$Ru(bpy)_2(mba\text{-}bpy)(PF_6)_2$: *m/z* 335.0795 $[C_{35}H_{32}N_6O_2Ru]^{2+}$ (calculated: 335.0810), *m/z* 815.1235 $[C_{35}H_{32}N_6O_2RuPF_6]^+$ (calculated: 815.1267) (**6**).

$Ru(bpy)_2(mab\text{-}bpy)(PF_6)_2$ *m/z* 946.0 $[C_{35}H_{36}N_7RuP_2F_{12}]^+$ (calculated: 945.7), *m/z* 800.1 $[C_{35}H_{35}N_7RuPF_6]^+$ (calculated: 799.74), *m/z* 928.1 $[C_{36}H_{36}N_6RuP_2F_{12}]^+$ (calculated: 928.7) (**7**).

Results and discussion

Spectroscopic properties

The UV-VIS spectra of compounds **0–7** are typical of ruthenium polypyridyl complexes. The UV region is dominated by spin allowed π–π* ligand-centered (LC) transitions while a broad lower intensity band appears at longer wavelengths assigned to a metal to ligand charge transfer (MLCT) (*i.e.* d → π* transition). The position of the MLCT band for the complexes in acetonitrile varied between 450 nm and 480 nm depending on the identity of the ligands (Table 1). Following optical excitation, the initially produced ^{1}MLCT rapidly decays through intersystem crossing to the corresponding triplet state (^{3}MLCT) with close to unit efficiency. For each of the complexes, intense luminescence resulted from the decay of this excited state. Fig. 2a shows the corrected photoluminescence spectra for $Ru(bpy)_3^{2+}$ and the derivatives containing attachment functionality (in deaerated CH_3CN at room temperature). The emission colour varied significantly depending on the nature of the substituents. The data presented in Table 1 show that there is a range of approximately 70 nm between the unsubstituted $Ru(bpy)_3^{2+}$ standard and the longest wavelength emitting ester derivatised complex. The *y*-axis has been normalised in Fig. 2a for the absorbance of each solution in order to emphasize the relative photoluminescence efficiencies (Φ_p) of the complexes. The values of Φ_p, using $Ru(bpy)_3^{2+}$ as a standard, varied between approximately 6% and 8% (Table 1).

Table 1 Spectroscopic data for the $[Ru(bpy)_2(L)]^{3+}$ complexes in acetonitrile

			Abs.	Photolumin.		ECL	
Complex number	Ligand		λ_{max}/ nm	λ_{max}/ nm[a]	Φ_p[b]	λ_{max}/ nm	Φ_{ECL}
0	bpy	—	451	618	0.062	620	0.050
7	mab-bpy	Alkyl	448	625	0.055	625	0.001
6	mba-bpy	Alkyl	454	629	0.074	630	0.040
4	Me-Ala-bpy-dc	Amide	469	668	0.085	666	0.065
3	dm-bpy-dc	Ester	478	686	0.061	685	0.049
5	men-bpy-dc	Ester	478	686	0.072	685	0.055

[a] Corrected. [b] Relative quantum yield (tris(2,2′-bipyridine)ruthenium-(II) = 0.062) (acetonitrile, room temperature, degassed).[45]

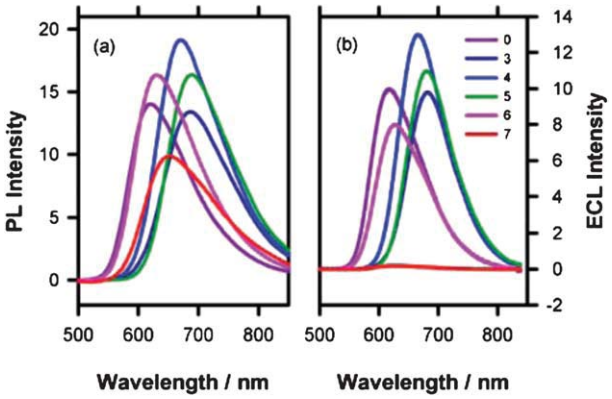

Fig. 2 Photoluminescence (a) and ECL spectra (b) of $[Ru(bpy)_2L]^{2+}$ complexes in acetonitrile. The ECL was generated using a glassy carbon electrode in a 1 mM solution of the complex containing 0.1 M $TBAPF_6$ supporting electrolyte. The *y*-axis in (a) is normalised for the photons absorbed while the *y*-axis in (b) is normalised for the electrons passed during the generation of the luminescence.

Electrochemistry

The electrochemical data are summarised in Table 2, while Fig. 3 shows representative cyclic voltammetric responses for three complexes: the butanoic acid (**6**), methyl (**1**), and ester (**5**) derivatives. All of the complexes exhibited voltammetric behaviour typical of ruthenium polypyridyl complexes. A single redox process corresponding to the Ru^{2+}/Ru^{3+} redox couple occurred at high positive potentials while three or more stepwise ligand reductions were observed in the negative region of the voltammogram. Reversible solution phase behaviour was observed for most processes, values of the diffusion coefficient (*D*) (see Table 2) in each case were evaluated from the slopes of plots of peak current *versus* square root of scan rate for the metal based redox couple.

Adding electron withdrawing ester functionality had a significant effect on the voltammetric response, resulting in a large positive shift in the first reduction potential. This is illustrated in Fig. 3 for complex **5**, which shows that the reduction process associated with the derivatised ligand was significantly displaced from the two subsequent bipyridine reductions. There was also a small positive shift in the formal potential of the Ru^{2+}/Ru^{3+} couple. By contrast, the ligand reductions remained evenly spaced and virtually unaffected by the methyl substitution in the case of complex **6** (Fig. 3), though there was a small negative shift in the metal oxidation potential. Fig. 4a and the data in Table 2

Table 2 Electrochemical data for the $[Ru(bpy)_2(L)]^{3+}$ complexes in acetonitrile

		E°/V (*vs.* Fc)					
Complex number	Ligand	I	II	III	IV	10^6 D/cm^2 s^{-1}	ΔE° (II − I)[a]/eV
0	bpy	0.892	−1.754	−1.937	−2.178	5.8	−2.65
1	dm-bpy	0.833	−1.759	−1.961	−2.211	7.3	−2.59
7	mab-bpy	0.833	−1.755	−1.954	−2.217	2.1	−2.59
6	mba-bpy	0.836	−1.756	−1.972	−2.233	4.3	−2.59
2	dc-bpy	0.996	(−1.494)	—	—	6.4	−2.49
4	Me-Ala-bpy-dc	0.967	−1.467	−1.861	−2.077	4.4	−2.43
3	dm-bpy-dc	0.983	−1.396	−1.857	−2.058	4.9	−2.38
5	men-bpy-dc	0.996	−1.385	−1.837	−2.036	4.9	−2.38

[a] ΔE° (II − I) represents the HOMO–LUMO gap or the free energy (ΔG) for the reaction between the oxidised, $[Ru(bpy)_2(L)]^{3+}$ and reduced $[Ru(bpy)_2(L)]^{+}$ forms of the complex.

Published on 04 February 2011 on http://pubs.rsc.org | doi:10.1039/C0AN00952K
Downloaded by Deakin University on 03 January 2012

show that these trends also apply to the other complexes studied. The carboxylate functionality on **2**, **3**, **4** and **5** significantly lowered the reduction potential relative to the unsubstituted complex (**0**), but only moderately increased the oxidation potential, with the ester producing a larger shift than the amide. In the case of **1** and **6**, the ligand based reductions were unaffected by the electron donating alkyl substituent, but the complexes are slightly more easily oxidised. Moreover, neither the alkyl chain length nor its end group had any effect on the redox potentials.

Electrochemical characteristics are often found to be a good predictor of spectroscopic properties.[12,76] In particular, the HOMO–LUMO gap is closely related to the difference in ground state redox potentials, ΔE° ($=E^\circ$(I) − E°(II), see Table 2). These values may be compared with the excited state energies from the photoluminescence data. Although the spectroscopic energy is more accurately estimated from the E_{0-0} band from the low temperature emission spectrum, it has been shown that for a series of related transition metal complexes the difference is constant.[12] Fig. 5 shows that there was excellent correlation between ΔE° and the energy corresponding to absorption or emission maxima. This implies that the orbitals involved in the electrochemical reactions are identical to those implicated in the MLCT absorption and π*–d emission processes. The slope of the linear fit (0.85) also supports this. The intercept of −130 mV arises for two reasons; firstly, as a consequence of the use of room

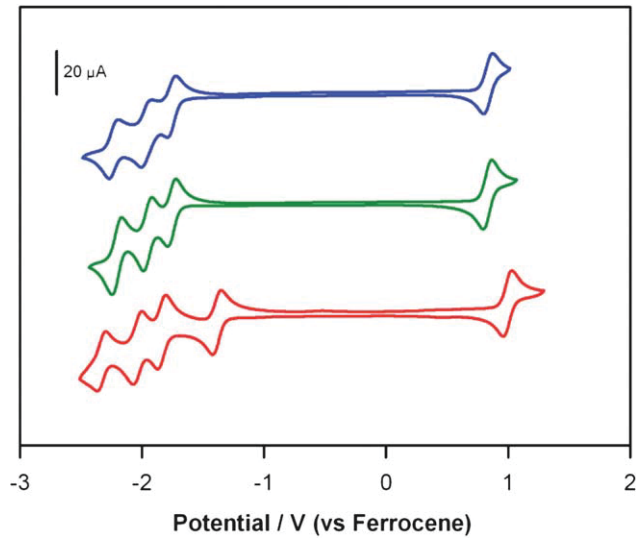

Fig. 3 Cyclic voltammetry of **6** (top), **1** (middle) and **5** (bottom) in CH_3CN containing 0.1 M $TBAPF_6$ at a 3 mm diameter GC electrode. In each case, the concentration of the complex was 1 mM and the scan rate was 0.1 V s^{-1}.

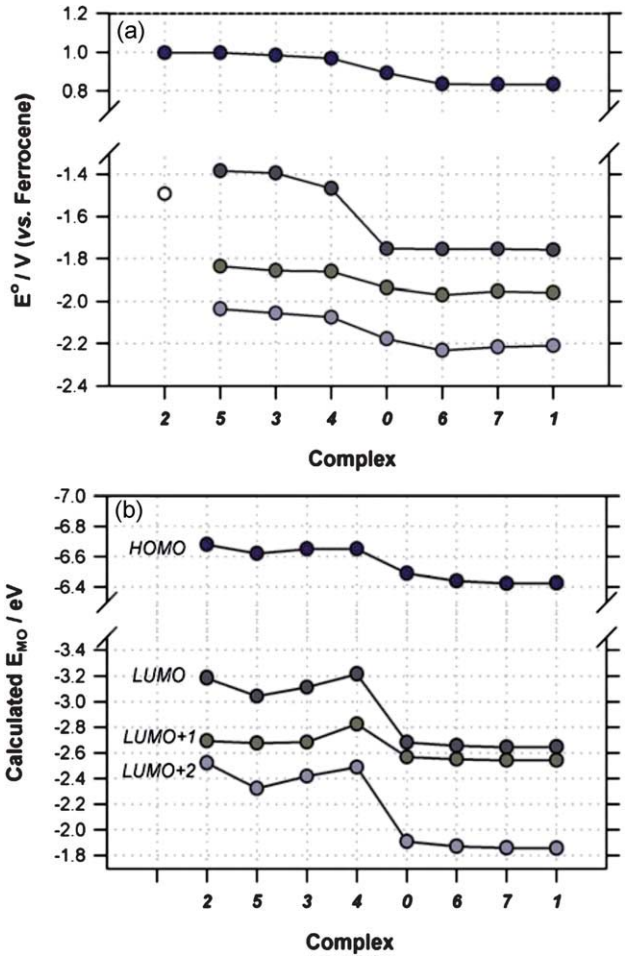

Fig. 4 Effect of substituents on the (a) electrochemical properties and (b) MO energies of $[Ru(bpy)_2(L)]^{2+}$, where L is the ligand indicated by the number of the complex on the *x*-axis. Experimental conditions as in Fig. 3. The open circle represents an irreversible wave. Calculated MO energies at the mPW1PW91/SDD level of theory with acetonitrile solvent.

This journal is © The Royal Society of Chemistry 2011

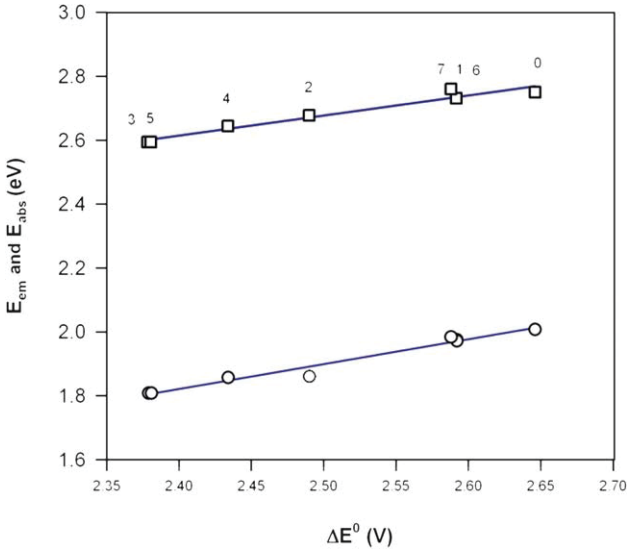

Fig. 5 Correlation of electrochemical with spectroscopic and DFT calculated data. ΔE° is the difference between the first oxidation and first reduction potentials. E_{em} (circles) and E_{abs} (squares) are the energies of the emission and absorption bands respectively. The DFT HOMO–LUMO gap is calculated from mPW1PW91/SDD orbital energies, including effect of acetonitrile solvent.

temperature spectroscopic data; and secondly from coulombic factors because of the different electronic configuration of the state produced by electrochemical reduction of the $[Ru(bpy)_2(L)]^{2+}$ complex, *i.e.* $(t_{2g})^6(\pi^*)^1$ and the spectroscopic excited state $(t_{2g})^5(\pi^*)^1$.

As the spectroscopic and redox orbitals are equivalent, this allows interpretation of the trends in emission wavelength with reference to the electrochemical data. Clearly, alkyl substitution had the smallest impact on the spectroscopic properties with the emission from **6** and **7** red shifted by up to 11 nm with respect to the unsubstituted standard, **0**. On the basis of the electrochemical data in Fig. 4 we can surmise that these groups have a small destabilising effect on the HOMO but scarcely impact on the energy of the LUMO at all. This is related to the low percentage contribution to the LUMO for the substituted ligands (L) for these particular complexes as shown in the next section.

On the other hand, amide or ester groups red shifted the emission by 50 to 70 nm. The electrochemical trends in Fig. 4 reveal that this occurred as a result of a significant stabilisation of the LUMO accompanied by a minor decrease in the energy of the HOMO. These data show that the colour of the luminescence can be tuned in these species without significantly altering the energy of the HOMO. This is an important conclusion because, to give efficient, analytically useful ECL, a luminophore also needs to be a strong oxidant, generally with a formal potential ~1 V *vs.* Ag/AgCl or greater. These experiments show that ECL active sensing materials could be designed to exhibit significantly different coloured emission for multiplexed detection while maintaining relatively constant redox ability.

Theoretical calculations

Initial calculations of HOMO–LUMO energies in the gas phase produced results with little correlation to experimental trends. In this work, the effect of solvation on MO energies, and in particular the HOMO–LUMO gap, was very significant. Inclusion of solvent effects yielded trends in much better agreement with experimental data. For this reason, only theoretical results including solvation effects are presented. The minimal LANL2MB basis set produced apparently spurious results, while the LANL2DZ and SDD results followed similar trends. Single-point energies with the TZVP basis (with SDD for Ru) yielded similar results to the 6-31+G(d) basis (SDD for Ru), with the TZVP calculated HOMO–LUMO gap consistently smaller by 0.02 eV. For the purpose of comparison with experimental data, only SDD/TZVP calculated results have been considered, although the SDD/6-31+G(d) results may equally have been used.

Plots of MO energies in Fig. 4 illustrate the similarity of trends between the calculated energies and the observed electrochemical properties. That is, two groups are formed with LUMOs of *ca.* −3.1 eV (**2–5**) and *ca.* −2.6 eV (**0**, **1**, **6**, **7**). The HOMO energy is reasonably consistent for all compounds. This grouping in LUMO energy is responsible for the significant increase in HOMO–LUMO gap that occurs between **4** and **0**, which is consistent with the experimental observation of a change in redox and spectroscopic properties between the same compounds. The actual values of the HOMO–LUMO gaps calculated by DFT and time dependent (TD) DFT are presented in the ESI† where they are compared with the corresponding spectroscopic and electrochemical data.

Mulliken population analysis of the frontier MOs (summarised in Fig. 6) serves to illustrate how the nature of the HOMO and LUMO explains the observed trends in spectroscopic and electrochemical properties. The population analyses are included in the ESI (Tables S2–S9†). For compounds **0**, **1**, **6**, and **7**, the LUMO is predominantly bpy in character, however, for compounds **2–5**, the LUMO is dominated by contributions from the modified ligand (L). In each case the HOMO contributions are reasonably consistent (about 80% Ru metal contribution). This analysis goes someway to confirming that we can 'tune' electrochemical and photophysical properties by 'tuning' the LUMO energy, as was our goal in this work.

Electrochemiluminescence

The ECL properties of ruthenium diimine complexes are well known. One pathway by which the emission can be produced is *via* potential step annihilation ECL experiments, where the electrode potential is alternated between values sufficiently positive to generate the 3+ form and sufficiently negative to generate the 1+ forms of the complex. This results in generation of the excited complex according to:

$$[Ru(bpy)_2(L)]^{2+} \rightarrow [Ru(bpy)_2(L)]^{3+} + e^- \quad (3)$$

$$[Ru(bpy)_2(L)]^{2+} + e^- \rightarrow [Ru(bpy)_2(L)]^{+} \quad (4)$$

$$[Ru(bpy)_2(L)]^{3+} + [Ru(bpy)_2(L)]^{+} \rightarrow [Ru(bpy)_2(L)]^{2+*} + [Ru(bpy)_2(L)]^{2+} \quad (5)$$

$$[Ru(bpy)_2(L)]^{3+} + [Ru(bpy)_2(L)]^{+} \rightarrow 2\,[Ru(bpy)_2(L)]^{2+} \quad (6)$$

$$[Ru(bpy)_2(L)]^{2+*} \rightarrow [Ru(bpy)_2(L)]^{2+} + h\nu \quad (7)$$

Published on 04 February 2011 on http://pubs.rsc.org | doi:10.1039/C0AN00952K
Downloaded by Deakin University on 03 January 2012

Published on 04 February 2011 on http://pubs.rsc.org | doi:10.1039/C0AN00952K
Downloaded by Deakin University on 03 January 2012

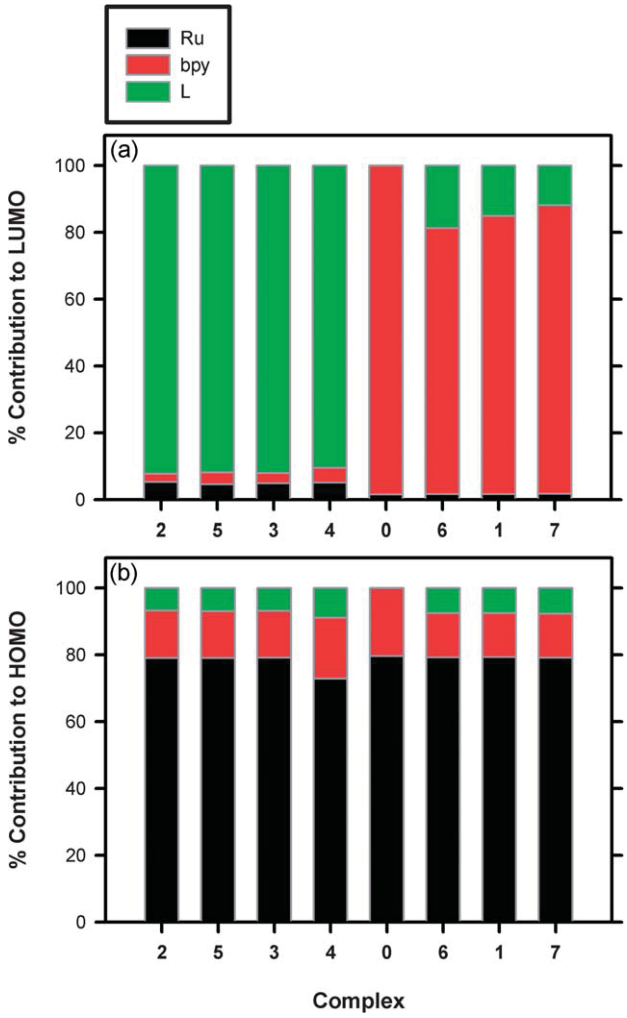

Fig. 6 Percentage contribution to HOMO and LUMO of metal centre (Ru), bipyridine ligands (bpy) and substituted ligand (L) in $[Ru(bpy)_2L]^{2+}$ complexes.

Although this annihilation mode of ECL is not typically used in sensing, it serves as a useful means to characterise the fundamental aspects of the ECL properties of luminophores because of the relative complexity of mechanisms involved in the co-reactant mode of ECL. For each of the complexes studied here, such annihilation experiments resulted in intense emission from the electrode surface that was easily visible with the naked eye. ECL efficiencies (Φ_{ECL}), defined as the number of photons emitted per electron transferred in reactions (5) and (6) above, were determined by comparing charge passed in the forward step to the integrated light intensity from the ECL spectrum collected during the reverse step, using eqn (2), with $Ru(bpy)_3^{2+}$ as a reference ($\Phi_{ECL} = 0.05$).[46]

Fig. 2b shows the ECL spectrum for each of the ruthenium complexes. The *y*-axis is normalised for the charge passed during the forward potential step of the experiment used to generate the emission. The relative heights of the peaks in this figure therefore reflect the relative ECL efficiencies of the complexes in an analogous manner to the absorbance normalised spectra in Fig. 2a. This figure and the data in Table 1 show that with the exception of complex **7** ($\Phi_{ECL} = 0.001$), the ECL efficiency Φ_{ECL} varies over quite a limited range (0.040 to 0.065) and each of the complexes has similar or slightly higher efficiencies than the parent complex, $Ru(bpy)_3^{2+}$.

In general, the efficiency of ECL emission is determined by a number of (sometimes competing) factors including the quantum yield of emission Φ_p according to:

$$\Phi_{ECL} = \Phi_{ex}\Phi_p \quad (8)$$

where Φ_{ex} is the efficiency associated with the production of the excited state. Thus Φ_{ECL} also depends on the competition between reactions leading to excited state and ground state and on the stability of the redox partners in reaction (5). Finally, Φ_{ECL} also depend on the free energy change associated with the annihilation reactions (5) and (6) above. Reaction (5) which produces an excited state (es) competes with the much more exergonic reaction (6) to ground state (gs). According to the Marcus theory of electron transfer, photons are produced because the rate of reaction (6) is kinetically inhibited depending on the extent of its exergonicity.

The values of ΔG_{gs} for reaction (6) are calculated from the redox potentials of the species involved and are numerically equal to the ΔE° (HOMO–LUMO gap) values given in Table 2. The values of ΔG_{es} for reaction (5) may be estimated using eqn (9):

$$\Delta G_{es} = \Delta E^\circ + E_{MLCT} \quad (9)$$

where E_{MLCT} is the spectroscopic energy of the excited state, which is best taken from the low temperature emission spectrum, but may be taken from room temperature data to a first approximation. Table 2 shows that the values of ΔG_{gs} ($=\Delta E^\circ$) vary between −2.38 and −2.66 eV. As these values exceed the excited state energies in each case, which vary between 1.81 eV for **5** and 2.01 eV for **0**, all of the ECL reactions are energy sufficient systems. Substituting these data into eqn (9) shows that values of ΔG_{es} vary over quite a narrow range between −0.59 eV and −0.65 eV. That no correlation is observed between Φ_{ECL} or Φ_{ex} and ΔG_{gs} or ΔG_{es} is perhaps not surprising given the narrow range of exergonicities; however, it is also clear that other factors apart from energetics come into play in determining the ECL intensity. In agreement with eqn (8), the value of Φ_{ECL} tracks Φ_p quite well in most cases; the efficiency of excited state production Φ_{ex} is 78 ± 3% for each compound excluding **6** and **7**. The butanoic acid functionalised complex **6** has the highest photoluminescence efficiency yet the lowest ECL efficiency, which we attribute to side reactions with the carboxylic acid that compete with reaction (5). Similarly, complex **7** has a pendant amine group, which may be directly oxidised at the electrode. In addition to degrading the overall efficiency of reaction (5), this is likely to interfere with ECL in other ways such as electrode passivation or quenching of the excited state.

Conclusions

The luminescence of tris(2,2′-bipyridine)ruthenium(II) derivatives (with functionality enabling coupling to other molecules or surfaces) can be spectrally tuned over a range of wavelengths by

 This journal is © The Royal Society of Chemistry 2011

varying the substituents at the 4 and 4′ positions of one of the bipyridine ligands. Alkyl groups tend to moderately destabilise the HOMO without affecting the LUMO. Amide or ester groups on the other hand moderately stabilise the HOMO but significantly stabilise the LUMO. The ability to tune the luminescence without significantly altering the energy of the HOMO (*i.e.* maintaining relatively constant redox ability) is important as it allows for the design of ECL probes with different coloured emission for applications such as multiplexed detection. DFT calculations showed that the LUMO is dominated by the substituted ligand for the complexes containing electron withdrawing substituents and by the unsubstituted bpy ligand for the complexes containing electron donating groups. Therefore, in addition to offering insights into their fundamental properties, DFT may be used to predict trends in redox and spectroscopic properties within a related set of complexes such as this. It is thus a potentially useful tool in the discovery of new ECL and CL active luminophores.

The electrochemical HOMO–LUMO gap is a good predictor of the spectroscopic properties. Excellent correlation was observed between the difference in ground state redox potentials, ΔE° (=II − I), and the energy corresponding to absorption or emission maxima. ECL intensity in general depends on a number of competing factors; if some of these can be held constant, ECL efficiency can be more easily predicted. The relationship between the exergonicity of the annihilation reaction leading to photon emission and Φ_{ECL} is well known.[77] Because the same factors that dictate ΔG for the annihilation reaction (*i.e.* the relative energies of the HOMO and LUMO) have a corresponding effect on the energy of the excited state product, the value of ΔG_{es} is relatively constant (0.61 ± 0.03 eV) for this series of complexes. Most of the complexes populate the excited state with an efficiency (Φ_{ex}) of close to 80% under the conditions used in this study, suggesting that the stability of the redox partners and the competition between reactions leading to excited state and ground state is about the same for most of the complexes. However, in the case of **6**, Φ_{ex} is only 54%, with the result that it has the second lowest ECL efficiency despite having the highest quantum yield. The low Φ_{ex} may be because the acid functionality introduces the possibility of competing side reactions. The ECL of the alkylamine complex **7**, which has a Φ_{ex} of only 2%, is even more dramatically affected because in addition to other possible side reactions the amine moiety may react with the carbon electrode itself resulting in passivation. Clearly, potentially reactive groups should be avoided in the design of ECL based sensing materials because of the possibility of side reactions occurring during or after the electrochemical step. It should be noted, however, that the effect of the reactive group is negated when it is used for labelling purposes, as demonstrated by the strong ECL observed for **4** where the carboxylic moiety has been used to couple the complex to an amino acid. Complexes **6** and **7** have served the purpose of illustrating a point in this study but it is acknowledged that their properties will be altered when used in a labelling or bioconjugation context. Despite the range of factors that may degrade the efficiency of population of the excited state, in general, the photoluminescence quantum yield (Φ_p) is a reasonable predictor of the ECL yield (Φ_{ECL}), within related sets of compounds such as this.

Published on 04 February 2011 on http://pubs.rsc.org | doi:10.1039/C0AN00952K
Downloaded by Deakin University on 03 January 2012

References

1 J. G. Vos and J. M. Kelly, *Dalton Trans.*, 2006, 4869–4883.
2 V. Balzani and A. Juris, *Coord. Chem. Rev.*, 2001, **211**, 97–115.
3 M. Grätzel, *Inorg. Chem.*, 2005, **44**, 6841–6851.
4 J. R. Lakowicz, *Principles of Fluorescence Spectroscopy*, Springer, New York, 3rd edn, 2006.
5 B. A. Gorman, P. S. Francis and N. W. Barnett, *Analyst*, 2006, **131**, 616–639.
6 M. M. Richter, *Chem. Rev.*, 2004, **104**, 3003–3036.
7 A. Juris, V. Balzani, F. Barigelletti, S. Campagna, P. Belser and A. Von Zelewsky, *Coord. Chem. Rev.*, 1988, **84**, 85–277.
8 V. Balzani, A. Juris, M. Venturi, S. Campagna and S. Serroni, *Chem. Rev.*, 1996, **96**, 759–833.
9 Y. Shen, B. P. Maliwal and J. R. Lakowicz, *J. Fluoresc.*, 2003, **13**, 163–168.
10 P. A. Mabrouk and M. S. Wrighton, *Inorg. Chem.*, 1986, **25**, 526–531.
11 D. Bruce, J. McCall and M. M. Richter, *Analyst*, 2002, **127**, 125–128.
12 G. Orellana, M. L. Quiroga and A. M. Braun, *Helv. Chim. Acta*, 1987, **70**, 2073–2086.
13 A. Börje, O. Köthe and A. Juris, *J. Chem. Soc., Dalton Trans.*, 2002, 843–848.
14 M. Zhou, G. P. Robertson and J. Roovers, *Inorg. Chem.*, 2005, **44**, 8317–8325.
15 W. R. Browne, P. Passaniti, M. T. Gandolfi, R. Ballardini, W. Henry, A. Guckian, N. O'Boyle, J. J. McGarvey and J. G. Vos, *Inorg. Chim. Acta*, 2007, **360**, 1183–1190.
16 T. Sajoto, P. I. Djurovich, A. B. Tamayo, J. Oxgaard, W. A. Goddard and M. E. Thompson, *J. Am. Chem. Soc.*, 2009, **131**, 9813–9822.
17 J. I. Kim, I.-S. Shin, H. Kim and J.-K. Lee, *J. Am. Chem. Soc.*, 2005, **127**, 1614–1615.
18 R. J. Forster, P. Bertoncello and T. E. Keyes, *Annu. Rev. Anal. Chem.*, 2009, **2**, 359–385.
19 S. F. McClanahan, R. F. Dallinger, F. J. Holler and J. R. Kincaid, *J. Am. Chem. Soc.*, 1985, **107**, 4853–4860.
20 S. J. Park, D. H. Kim, D. H. Kim, H. J. Park, D. N. Lee, B. H. Kim and W.-Y. Lee, *Anal. Sci.*, 2001, **17**, a93–a96.
21 N. W. Barnett, R. Bos, H. Brand, P. Jones, K. F. Lim, S. D. Purcell and R. A. Russell, *Analyst*, 2002, **127**, 455–458.
22 J.-K. Lee, S.-H. Lee, M. Kim, H. Kim, D.-H. Kim and W.-Y. Lee, *Chem. Commun.*, 2003, 1602–1603.
23 A. Macatangay, G. Y. Zheng, D. P. Rillema, D. C. Jackman and J. W. Merkert, *Inorg. Chem.*, 1996, **35**, 6823–6831.
24 L. Della Ciana, I. Hamachi and T. J. Meyer, *J. Org. Chem.*, 1989, **54**, 1731–1735.
25 M. Staffilani, E. Höss, U. Giesen, E. Schneider, F. Hartl, H.-P. Josel and L. De Cola, *Inorg. Chem.*, 2003, **42**, 7789–7798.
26 D. N. Lee, J. K. Kim, H. S. Park, Y. M. Jun, R. Y. Hwang, W.-Y. Lee and B. H. Kim, *Synth. Met.*, 2005, **150**, 93–100.
27 S. Anderson, E. C. Constable, K. R. Seddon, J. E. Turp, J. E. Baggott and M. J. Pilling, *J. Chem. Soc., Dalton Trans.*, 1985, 2247–2261.
28 P.-H. Xie, Y.-J. Hou, B.-W. Zhang, Y. Cao, F. Wu, W.-J. Tian and J.-C. Shen, *J. Chem. Soc., Dalton Trans.*, 1999, 4217–4221.
29 E. Eskelinen, S. Luukkanen, M. Haukka, M. Ahlgrén and T. A. Pakkanen, *J. Chem. Soc., Dalton Trans.*, 2000, 2745–2752.
30 V. Aranyos, J. Hjelm, A. Hagfeldt and H. Grennberg, *Dalton Trans.*, 2003, 1280–1283.
31 P. Pearson, A. M. Bond, G. B. Deacon, C. Forsyth and L. Spiccia, *Inorg. Chim. Acta*, 2008, **361**, 601–612.
32 G. F. Strouse, P. A. Anderson, J. R. Schoonover, T. J. Meyer and F. R. Keene, *Inorg. Chem.*, 1992, **31**, 3004–3006.
33 H. Wang, C. Zhang, Y. Li and H. Qi, *Anal. Chim. Acta*, 2006, **575**, 205–211.
34 M. Buda, F. G. Gao and A. J. Bard, *J. Solid State Chem.*, 2004, **8**, 706–717.
35 D. Hesek, Y. Inoue, H. Ishida, S. R. L. Everitt and M. G. B. Drew, *Tetrahedron Lett.*, 2000, **41**, 2617–2620.
36 K. Ohkubo, M. Fukushima, H. Ohta and S. Usui, *J. Photochem. Photobiol., A*, 1996, **98**, 137–140.
37 D. N. Lee, B. K. Soh, S. H. Kim, Y. M. Jun, S. H. Yoon, W.-Y. Lee and B. H. Kim, *J. Organomet. Chem.*, 2008, **693**, 655–666.
38 E. S. Handy, A. J. Pal and M. F. Rubner, *J. Am. Chem. Soc.*, 1999, **121**, 3525–3528.
39 E. Yavin, L. Weiner, R. Arad-Yellin and A. Shanzer, *J. Phys. Chem. A*, 2004, **108**, 9274–9282.

View Online

40 M. Suzuki, C. C. Waraksa, T. E. Mallouk, H. Nakayama and K. Hanabusa, *J. Phys. Chem. B*, 2002, **106**, 4227–4231.
41 W. Miao, J.-P. Choi and A. J. Bard, *J. Am. Chem. Soc.*, 2002, **124**, 14478–14485.
42 G. M. Greenway, A. Greenwood, P. Watts and C. Wiles, *Chem. Commun.*, 2006, 85–87.
43 F. Szemes, D. Hesek, Z. Chen, S. W. Dent, M. G. B. Drew, A. J. Goulden, A. R. Graydon, A. Grieve, R. J. Mortimer, T. Wear, J. S. Weightman and P. D. Beer, *Inorg. Chem.*, 1996, **35**, 5868–5879.
44 D. Hesek, Y. Inoue, S. R. L. Everitt, H. Ishida, M. Kunieda and M. G. B. Drew, *Inorg. Chem.*, 2000, **39**, 308–316.
45 J. V. Caspar and T. J. Meyer, *J. Am. Chem. Soc.*, 1983, **105**, 5583–5590.
46 W. L. Wallace and A. J. Bard, *J. Phys. Chem.*, 1979, **83**, 1350–1357.
47 M. J. Frisch, G. W. Trucks, H. B. Schlegel, G. E. Scuseria, M. A. Robb, J. R. Cheeseman, G. Scalmani, V. Barone, B. Mennucci, G. A. Petersson, H. Nakatsuji, M. Caricato, X. Li, H. P. Hratchian, A. F. Izmaylov, J. Bloino, G. Zheng, J. L. Sonnenberg, M. Hada, M. Ehara, K. Toyota, R. Fukuda, J. Hasegawa, M. Ishida, T. Nakajima, Y. Honda, O. Kitao, H. Nakai, T. Vreven, J. J. A. Montgomery, J. E. Peralta, F. Ogliaro, M. Bearpark, J. J. Heyd, E. Brothers, K. N. Kudin, V. N. Staroverov, R. Kobayashi, J. Normand, K. Raghavachari, A. Rendell, J. C. Burant, S. S. Iyengar, J. Tomasi, M. Cossi, N. Rega, J. M. Millam, M. Klene, J. E. Knox, J. B. Cross, V. Bakken, C. Adamo, J. Jaramillo, R. Gomperts, R. E. Stratmann, O. Yazyev, A. J. Austin, R. Cammi, C. Pomelli, J. W. Ochterski, R. L. Martin, K. Morokuma, V. G. Zakrzewski, G. A. Voth, P. Salvador, J. J. Dannenberg, S. Dapprich, A. D. Daniels, Ö. Farkas, J. B. Foresman, J. V. Ortiz, J. Cioslowski and D. J. Fox, *Gaussian 09, Revision A.1*, Gaussian, Inc., Wallingford CT, 2009.
48 A. D. Becke, *J. Chem. Phys.*, 1993, **98**, 5648–5652.
49 A. D. Becke, *Phys. Rev. A*, 1988, **38**, 3098–3100.
50 C. Lee, W. Yang and R. G. Parr, *Phys. Rev. B: Condens. Matter*, 1988, **37**, 785–789.
51 C. Adamo and V. Barone, *J. Chem. Phys.*, 1998, **108**, 664–675.
52 J. P. Perdew, in *Electronic Structure of Solids '91*, ed. P. Ziesche and H. Eschrig, Akademie Verlag, Berlin, 1991, pp. 11–20.
53 J. Lin, K. Wu and M. Zhang, *J. Comput. Chem.*, 2009, **30**, 2056–2063.
54 W. J. Hehre, R. F. Stewart and J. A. Pople, *J. Chem. Phys.*, 1969, **51**, 2657–2664.
55 J. B. Collins, P. v. R. Schleyer, J. S. Binkley and J. A. Pople, *J. Chem. Phys.*, 1976, **64**, 5142–5151.
56 P. J. Hay and W. R. Wadt, *J. Chem. Phys.*, 1985, **82**, 270–283.
57 T. H. Dunning, Jr and P. J. Hay, in *Modern Theoretical Chemistry*, ed. H. F. Schaefer, III Plenum, New York, 1976, vol. 3, pp. 1–28.
58 D. Andrae, U. Haeussermann, M. Dolg, H. Stoll and H. Preuss, *Theor. Chim. Acta*, 1990, **77**, 123–141.
59 W. J. Hehre, R. Ditchfield and J. A. Pople, *J. Chem. Phys.*, 1972, **56**, 2257–2261.
60 T. Clark, J. Chandrasekhar, G. W. Spitznagel and P. v. R. Schleyer, *J. Comput. Chem.*, 1983, **4**, 294–301.
61 P. C. Hariharan and J. A. Pople, *Theor. Chim. Acta*, 1973, **28**, 213–222.
62 A. Schaefer, H. Horn and R. Ahlrichs, *J. Chem. Phys.*, 1992, **97**, 2571–2517.
63 A. Schaefer, C. Huber and R. Ahlrichs, *J. Chem. Phys.*, 1994, **100**, 5829–5835.
64 J. Tomasi, B. Mennucci and R. Cammi, *Chem. Rev.*, 2005, **105**, 2999–3093.
65 R. E. Stratmann, G. E. Scuseria and M. J. Frisch, *J. Chem. Phys.*, 1998, **109**, 8218–8224.
66 S. I. Gorelsky, *AOMix: Program for Molecular Orbital Analysis, Version 6.46*, University of Ottawa, 2010, http://www.sg-chem.net/.
67 G. M. Badger and W. H. F. Sasse, *J. Chem. Soc.*, 1956, 616–620.
68 W. H. F. Sasse and C. P. Whittle, *J. Chem. Soc.*, 1961, 1347–1350.
69 *Spectral Database for Organic Compounds SDBS*, National Institute of Advanced Industrial Science and Technology (AIST), Japan, 2008, http://riodb01.ibase.aist.go.jp/sdbs/cgi-bin/direct_frame_top.cgi.
70 A. R. Oki and R. J. Morgan, *Synth. Commun.*, 1995, **25**, 4093–4097.
71 A. Launikonis, P. A. Lay, A. W. H. Mau, A. M. Sargeson and W. H. F. Sasse, *Aust. J. Chem.*, 1986, **39**, 1053–1062.
72 G. Sprintschnik, H. W. Sprintschnik, P. P. Kirsch and D. G. Whitten, *J. Am. Chem. Soc.*, 1977, **99**, 4947–4954.
73 L. Della Ciana, W. J. Dressick and A. Von Zelewsky, *J. Heterocycl. Chem.*, 1990, **27**, 163–165.
74 B. P. Sullivan, D. J. Salmon and T. J. Meyer, *Inorg. Chem.*, 1978, **17**, 3334–3341.
75 H. D. Abruña, T. J. Meyer and R. W. Murray, *Inorg. Chem.*, 1979, **18**, 3233–3240.
76 D. P. Rillema, G. Allen, T. J. Meyer and D. Conrad, *Inorg. Chem.*, 1983, **22**, 1617–1622.
77 A. Kapturkiewicz and P. Szrebowaty, *J. Chem. Soc., Dalton Trans.*, 2002, 3219–3225.

Published on 04 February 2011 on http://pubs.rsc.org | doi:10.1039/C0AN00952K
Downloaded by Deakin University on 03 January 2012

 This journal is © The Royal Society of Chemistry 2011